EUROPHYSICS LETTERS

OFFPRINT

Vol. 66 • Number 4 • pp. 579–584

Phase coherence and the Nernst effect at magic angles in organic conductors

* * *

N. P. Ong, Weida Wu, P. M. Chaikin and P. W. Anderson

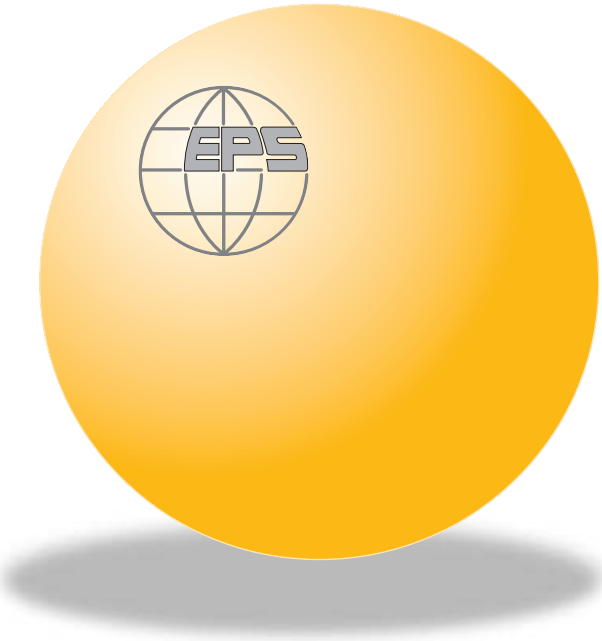

Published under the scientific responsibility of the
EUROPEAN PHYSICAL SOCIETY
Incorporating
JOURNAL DE PHYSIQUE LETTRES • LETTERE AL NUOVO CIMENTO

EDP SCIENCES

EUROPHYSICS LETTERS

Europhysics Letter was launched more than fifteen years ago by the European Physical Society, the Société Française de Physique, the Società Italiana di Fisica and the Institute of Physics (UK) and owned now by 17 National Physical Societies/Institutes.

Europhysics Letters aims to publish short papers containing non-trivial new results, ideas, concepts, experimental methods, theoretical treatments, etc. which are of broad interest and importance to one or several sections of the physics community.

Europhysics letters provides a platform for scientists from all over the world to offer their results to an international readership.

EUROPHYSICS LETTERS 15 May 2004

Europhys. Lett., **66** (4), pp. 579–584 (2004)
DOI: 10.1209/epl/i2004-10017-9

Phase coherence and the Nernst effect at magic angles in organic conductors

N. P. Ong, Weida Wu, P. M. Chaikin and P. W. Anderson
Department of Physics, Princeton University - Princeton, NJ 08544, USA

(received 1 March 2004; accepted 17 March 2004)

PACS. 74.20.-z – Theories and models of superconducting state.
PACS. 74.70.Kn – Organic superconductors.
PACS. 72.15.Jf – Thermoelectric and thermomagnetic effects.

Abstract. – A giant Nernst signal was recently observed for fields near crystallographic directions in $(TMTSF)_2PF_6$. Such large Nernst signals are most naturally associated with the motion of pancake vortices. We propose a model in which phase coherence is destroyed throughout the sample except in planes closely aligned with the applied field $\boldsymbol{H}$. A small tilt above or below the plane changes the direction and density of the penetrating vortices and leads to a Nernst signal that varies with the tilt angle of $\boldsymbol{H}$ as observed. The resistance notches at magic angles are understood in terms of flux-flow dissipation from field-induced vortices.

At low temperatures, the quasi–one-dimensional organic conductor $(TMTSF)_2PF_6$ displays a rich assortment of electronic phases, from spin-density-wave (SDW) to superconductivity to the field-induced spin-density-wave–quantum Hall effect (FISDW), as the applied pressure and magnetic field are varied [1–4]. For example, at a fixed pressure $P = 9\,\mathrm{kbar}$, $(TMTSF)_2PF_6$ is a superconductor in zero field at temperatures T below $T_c = 1.2\,\mathrm{K}$. In a moderate field $\boldsymbol{H}$, the zero-resistance state is destroyed in favor of a putative "metallic" state with large angular magnetoresistance. At larger fields, a cascade of phase transitions to semi-metallic and at the highest fields to an insulating FISDW state occurs. A striking feature in the metallic state is the existence of sharp notch anomalies in the resistance when $\boldsymbol{H}$ is aligned with the "magic angles" [1–4]. Lebed [5] originally predicted magic-angle effects with resistance peaks. However, resistance minima are observed instead. The origin of the magic-angle anomalies is an open problem despite a large number of proposed models [6, 7]. Recently, Wu, Lee and Chaikin (WLC) [8] uncovered a remarkable angular Nernst effect in the metallic state of $(TMTSF)_2PF_6$. The unusual angular dependence and the large magnitude of the Nernst signal (fig. 1) seem incompatible with the conventional transport theories. Here we show that a large resonant Nernst signal at the magic angles can result from phase slip and the partial restoration of long-range phase coherence of the superconducting pairing condensate when $\boldsymbol{H}$ is exactly aligned with a set of crystal planes.

Conventionally, the Nernst effect corresponds to the appearance of a transverse electric field $\boldsymbol{E}_N$ that is antisymmetric in both $\boldsymbol{H}$ and the applied temperature gradient $-\vec{\nabla}T$, *i.e.* $\boldsymbol{E}_N \sim \boldsymbol{H} \times \vec{\nabla}T$ (for, *e.g.*, $\boldsymbol{E}_N || \hat{\boldsymbol{z}}$ if $-\vec{\nabla}T || \hat{\boldsymbol{x}}$ and $\boldsymbol{H} || \hat{\boldsymbol{y}}$) [9, 10]. We refer to $e_N \equiv E_N/|\vec{\nabla}T|$ as

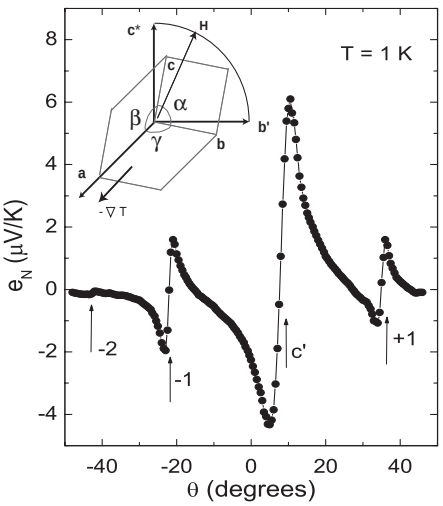

Fig. 1

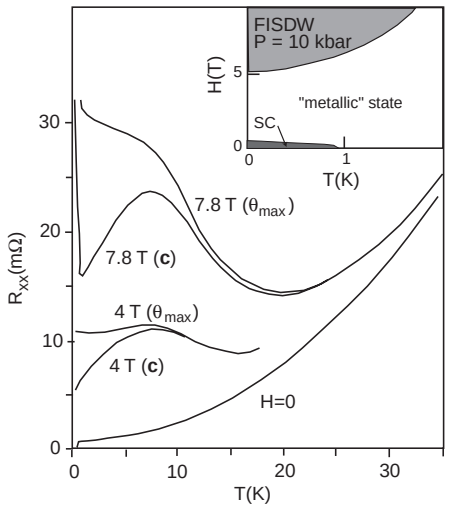

Fig. 2

Fig. 1 – The Nernst signal $e_{\rm N}$ *vs.* tilt angle θ in $(TMTSF)_2PF_6$ measured with $H = 7.5\,\mathrm{T}$, $T = 1\,\mathrm{K}$ and $P = 10\,\mathrm{kbar}$ (here $-\vec{\nabla}T||\boldsymbol{c}$ and $\boldsymbol{E}_{\rm N}||\boldsymbol{a}$). $e_{\rm N}$ changes sign at the magic angles θ_{-L1}, θ_c and θ_{L1}. The inset shows the standard experimental arrangement in which $-\vec{\nabla}T||\hat{\boldsymbol{x}}||\boldsymbol{a}$, $\hat{\boldsymbol{y}}||\boldsymbol{b}$ and $\hat{\boldsymbol{z}}||\boldsymbol{c}^*$, with reciprocal vectors $\boldsymbol{b}^*||\boldsymbol{c}\times\boldsymbol{a}$ and $\boldsymbol{c}^*||\boldsymbol{a}\times\boldsymbol{b}$. The field tilt angle θ is measured from the direction $\boldsymbol{c}^*$.

Fig. 2 – The T-dependence of R_{xx} measured at $H = 0, 4$, and $7.8\,\mathrm{T}$. Curves with $\boldsymbol{H}||\boldsymbol{c}'$ are compared with those measured with $\boldsymbol{H}$ in a local-maximum direction ($\theta_{\rm max}$) (adapted from ref. [4]). The inset is a schematic of the phase diagram in the H-T plane at $P = 10\,\mathrm{kbar}$. Superconductivity (SC) with long-range phase coherence is confined to the darker shaded region. We propose that $|\hat{\psi}(\boldsymbol{r})|$ survives in the chains deep into the metallic state.

the Nernst signal. In the experiment of WLC [8], $\boldsymbol{H}$ is rotated in the b^*c^* plane (the plane normal to $\boldsymbol{a}$; see fig. 1, inset). In the metallic state of $(TMTSF)_2PF_6$, they observed that, as θ is varied, the curve of $e_{\rm N}$ *vs.* θ is comprised of a series of sharp resonant-like curves centered at the magic angles (fig. 1).

Several features of the Nernst experiment are noteworthy. As noted, in conventional Nernst experiments, $E_{\rm N}$ changes its sign like the cross-product $\boldsymbol{H}\times\vec{\nabla}T$. By contrast, the sign-change in $e_{\rm N}$ at the magic angles in fig. 1 occurs even though neither $\boldsymbol{H}$ nor $\vec{\nabla}T$ changes sign as θ crosses a magic angle. Here, the sign of $e_{\rm N}$ reflects rather the component of $\boldsymbol{H}$ normal to a crystal plane, *e.g.* $\boldsymbol{H}\times\boldsymbol{c}'$ (a similar dependence of the magnetoresistance on $\boldsymbol{H}\times\boldsymbol{c}'$ was previously noted). Equally puzzling, the peak magnitude of $e_{\rm N}$ at $T \leq 1\,\mathrm{K}$ is 10^3–10^5 times larger than that derived from quasiparticle currents calculated from the band structure of $(TMTSF)_2PF_6$. Moreover, the peak signal increases rapidly as T decreases from 4 to 1 K, whereas a quasiparticle signal should decrease monotonically. Lastly, the large Nernst signal occurs in the face of an undetectably small thermopower S. This is anomalous for charge carriers because their drift velocity component $||(-\vec{\nabla}T)$ is generally much larger than the transverse component produced by the Lorentz force (*i.e.*, $S \gg e_{\rm N}$) [10]. By contrast, vortex flow $||(-\vec{\nabla}T)$ produces an E field that is predominantly transverse. Hence $e_{\rm N} \gg S$ (as observed) is a strong clue that the Nernst signal originates from vortex flow rather than charge carriers.

For the pressure P (7–10 kbar) and field (4–8 T) employed, $(TMTSF)_2PF_6$ is in the "metallic" state, which falls between the superconducting state (in which long-range phase coherence

is fully established) and the FISDW state (fig. 2, inset). We propose that, over large regions of the "metallic" state, the Cooper-pairing amplitude $|\hat{\psi}(\boldsymbol{r})|$ remains large within each chain along $\boldsymbol{a}$ but long-range phase coherence is absent for general field directions. The Nernst signal arises from phase slippage caused by vortex flow in these planes as $\boldsymbol{H}$ tilts off alignment.

In a type-II superconductor with extreme anisotropy and small superfluid density $\rho_{\rm s}$ (due to low carrier density), superfluidity (long-range phase coherence) is easily destroyed by strong non-Gaussian fluctuations of the phase $\varphi(\boldsymbol{r})$ in zero field even if $|\hat{\psi}|$ remains large [11]. In finite field, loss of long-range phase coherence at the vortex solid-to-liquid transition leads to a strongly dissipative vortex liquid state. The sharp increase in resistance at the melting line is often mistaken for the upper critical field. A series of experiments [10, 12–16] show that the vortex liquid state in cuprates is indistinguishable from the normal state by resistance measurements, but may be detected in a Nernst experiment. The persistence of the vortex liquid state to regions of the phase diagram high above the Meissner state boundary may be easily missed using resistivity data alone.

Our starting assumption is that, in the "metallic" state of $(\mathrm{TMTSF})_2\mathrm{PF}_6$, loss of phase coherence arises from highly mobile 2D vortices living on the principal crystal planes ab, ac or $a(c \pm b)$. (The transfer integrals t_i in the 3 principal bond directions are in the ratio $t_a : t_b : t_c = 1 : 0.1 : 0.003$ [1]. Accordingly, the pairing strength is largest along $\boldsymbol{a}$, but progressively weaker along the bond directions $\boldsymbol{b}$, $\boldsymbol{c}$, $(\boldsymbol{c}-\boldsymbol{b})$ and $(\boldsymbol{c}+\boldsymbol{b})$ [2].) In a field $\boldsymbol{H}$ at finite T, the vortex population is comprised of thermally generated and field-induced vortices (fig. 3). Both the vorticity and population of the field-induced vortices are determined by $B_n \equiv \hat{\boldsymbol{n}} \cdot \boldsymbol{B}$, where $\hat{\boldsymbol{n}}$ is the unit vector normal to a principal plane and $\boldsymbol{B}$ the induction field. If $\boldsymbol{H}$ is exactly aligned with the plane, we have only thermally generated pairs of "up" and "down" vortices. (Planes not aligned with H are saturated with vortices to the extent that they have lost phase coherence.) Tilting $\boldsymbol{H}$ slightly out of the plane (fig. 3) leads to a steep increase in the field-induced population equal to $\boldsymbol{B} \cdot \hat{\boldsymbol{n}}$, and an increase in the resistance R_{xx} as displayed in fig. 2.

The flow of vortices parallel to $-\vec{\nabla}T$ leads naturally to a Nernst signal that changes sign with $\boldsymbol{B} \cdot \hat{\boldsymbol{n}}$ as observed by WLC [8]. We consider the case when $\boldsymbol{H}$ is close to alignment with the ac plane (*i.e.* $\boldsymbol{H}||\boldsymbol{c}'$ at the magic angle θ_c, fig. 3). The gradient $-\vec{\nabla}T||\boldsymbol{a}$ produces a vortex flow in this plane with velocity $\boldsymbol{v}||\boldsymbol{a}$. The passage of each vortex across a line $\perp \boldsymbol{a}$ causes a phase slip of 2π. By the Josephson equation, the rate of phase slippage $\dot{\varphi}$ leads to an electro-chemical potential difference between the two ends of the line $V_J = \hbar\dot{\varphi}/2e$, which translates to a Nernst electric field $\boldsymbol{E}_{\rm N} = B_n \hat{\boldsymbol{n}} \times \boldsymbol{v}$. Clearly, as we tilt $\boldsymbol{H}$ from just above the plane to just below it, $E_{\rm N}$ changes sign with B_n (fig. 3).

We estimate the magnitude of $e_{\rm N}$ as follows. The gradient exerts a line force $s_\phi(-\vec{\nabla}T)$ on each vortex, where s_ϕ is the "transport line entropy" [9, 10]. Equating this to the frictional damping force $\eta\boldsymbol{v}$, we have $v = s_\phi(-\vec{\nabla}T)/\eta$, with η the damping parameter. With $B_n \sim (\theta - \theta_c)B$, we have for the Nernst electric field along $\boldsymbol{c}$

$$E_{\rm N} = (\theta - \theta_c)B\frac{s_\phi}{\eta}\big[-\vec{\nabla}T\big] \quad (\theta \sim \theta_c). \tag{1}$$

In effect, as $\delta\theta = \theta - \theta_c$ changes sign, the field-induced vortices decrease in number to zero, and then reappear with the opposite circulation. Since $\boldsymbol{v}||(-\vec{\nabla}T)$ is unchanged, the Nernst signal changes in sign.

At small $|\delta\theta|$, the resistance and $E_{\rm N}$ both vary linearly with B_n. When these two quantities scale in the same way with field, their magnitudes are related through the damping parameter η. By eqs. (1) and (2) (see below), we have $\partial e_{\rm N}/\partial B_n = s_\phi/\eta$ and $\partial\rho_c/\partial B_n = \phi_0/\eta$, respectively, with ϕ_0 the flux quantum. We adopt the value $s_\phi \sim 1\ k_{\rm B}$ per 2D vortex inferred from

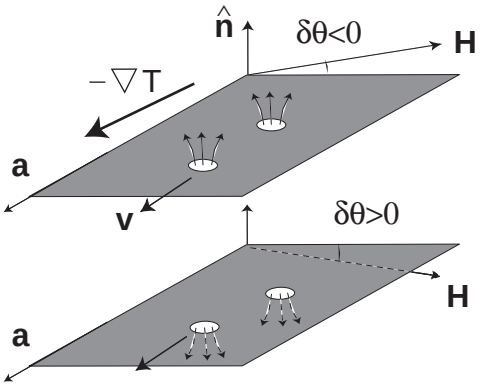

Fig. 3

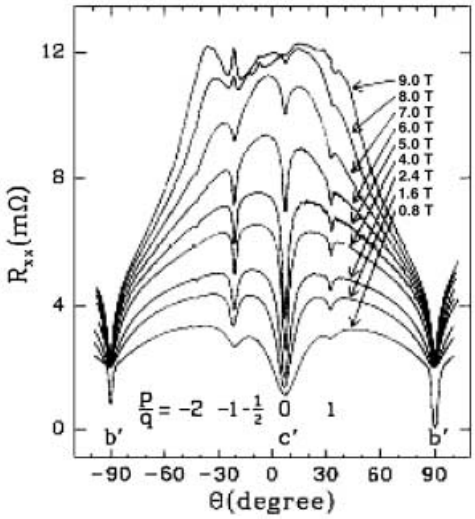

Fig. 4

Fig. 3 – Sketch of pancake vortices (circles with directed flux lines) created by $\boldsymbol{H}$ when it is near alignment with a plane (shaded surface). The density of vortices equals $\boldsymbol{B} \cdot \hat{\boldsymbol{n}}$. Phase slippage from the flow of vortices parallel to $-\vec{\nabla}T$ induces a large Nernst signal $e_{\rm N}$. As $\boldsymbol{H}$ tilts below the plane, $\boldsymbol{B} \cdot \hat{\boldsymbol{n}}$ and the vorticity change sign (lower sketch). Hence $e_{\rm N}$ also changes sign.

Fig. 4 – The angular dependence of R_{xx} in $(TMTSF)_2PF_6$ at 0.5 K with $P = 10$ kbar, at selected fields. Sharp notches in R_{xx} occur at the magic angles (ref. [1]).

experiments on cuprates [13]. From the results of Wu *et al.* at $H = 7$ T and $T = 1$ K [8], ρ_c is $\simeq 3\,\Omega$ cm at θ_c, which implies $\partial\rho_c/\partial\theta = 3.8 \times 10^{-6}\ \Omega$ m/deg. Using this and $s_\phi/\phi_0 \simeq 9$ A/K m, we find $\partial e_{\rm N}/\partial\theta \simeq 30\ \mu$V(K)$^{-1}$. We estimate a peak value $e_{\rm N} \simeq 200\ \mu$V/K when $\boldsymbol{E}_{\rm N}$ is measured along $\boldsymbol{c}$ in a gradient $||\boldsymbol{a}$ consistent with measurements. If, however, $\boldsymbol{E}_{\rm N}$ is measured along $\boldsymbol{a}$ with $\vec{\nabla}T||\boldsymbol{c}$ (as in the main panel in fig. 1), we should scale with the resistive notch in $\rho_a \sim 20\ \mu\Omega$ cm. This gives a peak $e_{\rm N} \simeq 2\ \mu$V/K, which is again consistent with experiment. As noted, calculations [8] of the Nernst signal produced by charge carriers are too small by a factor of 10^3–10^5 at 1 K.

When $|\delta\theta|$ exceeds 15°, ρ_a saturates to the normal-state dome-shaped background as phase coherence is reduced to short length scales. The Nernst signal reaches a peak near this tilt angle, and falls monotonically until θ reaches the next magic angle. (The peaking of the Nernst signal at a field close to where the resistance saturates is closely similar to what is observed in a recent experiment on cuprates [14].) The concatenation of such dispersion-like curves at successive magic angles accounts for the curve in fig. 1.

As the vortex velocity $\boldsymbol{v}$ is nearly parallel with $-\vec{\nabla}T$, the component of $\boldsymbol{E}_{\rm N}$ along $\boldsymbol{a}$ (which is detected as a thermopower signal) is negligible. This readily explains why S remains unresolvably small even as $e_{\rm N}$ increases to very large values with decreasing T.

The T-dependence of the Nernst signal is also consistent with a vortex origin. As T decreases from 4 K to 0.5 K, $e_{\rm N}$ increases dramatically by ~ 10 at θ_c (and even more steeply at $\theta_{\pm L1}$) [8]. This behavior is incompatible with charge carriers (for which both $e_{\rm N}$ and S decrease monotonically with T). For a vortex liquid, the T-dependence of $e_{\rm N}(T, H)$ is most well studied in underdoped $La_{2-x}Sr_xCuO_4$. There, as T decreases from 80 K in fixed H, $e_{\rm N}$ rises rapidly, continuing to do so below the zero-field critical temperature $T_{\rm c0} = 28$ K (fig. 1 of ref. [16]). At

lower T, $e_{\rm N}(T,H)$ attains a prominent maximum at $T_{\rm p}$, and then decreases rapidly to zero as the vortex-to-solid melting temperature $T_{\rm M}$ is approached ($T_{\rm M} < T_{\rm p} < T_{\rm c0}$). We expect that, near each magic-angle direction in $(TMTSF)_2PF_6$, $e_{\rm N}$ eventually rises to a peak before decreasing rapidly to zero as the 2D vortices approach solidification below 0.5 K. As $t_c > t_{c\pm b}$, the peak should occur at a higher T with $\boldsymbol{H}||\boldsymbol{c}$ (at θ_c) than with $\boldsymbol{H}||(\boldsymbol{c}\pm\boldsymbol{b})$ ($\theta_{\pm L1}$).

The 2D vortex model may also explain why sharp resistance minima are observed at the magic angles (fig. 4). We assume $\boldsymbol{H}$ is precisely aligned with the ac plane. Within the plane, phase coherence of the superconducting order parameter $|\psi(\boldsymbol{r})|e^{i\varphi(\boldsymbol{r})}$ extends to the Kosterlitz-Thouless (KT) correlation length ξ_+, which measures the spacing between thermally generated vortices (of density n_f). The area of the average phase-correlated region ξ_+^2 dictates the magnitude of the superfluid conductivity enhancement $\sigma_{\rm s}$. For an isotropic plane, Halperin and Nelson [17] derived $\sigma_{\rm s} = \sigma^{(\rm n)}/n_f 2\pi\xi^2$, with $\sigma^{(\rm n)}$ the normal-state resistance, and ξ the Ginzburg-Landau coherence length evaluated at $T_{\rm c}$. As shown in fig. 3, tilting $\boldsymbol{H}$ slightly away from θ_c produces 2D vortices of density $n_B = |H\sin\delta\theta|/\phi_0$ in that plane. The mobile field-induced vortices dramatically shrink the phase-correlated area, and result in a steep suppression of $\sigma_c^{(\rm s)}$. Hence, for small $\delta\theta$, we may write for the a-axis resistivity

$$\rho_a^{(\rm s)} = \rho_a^{(\rm n)} 2\pi(\xi_a\xi_c)\left(n_f + \frac{H}{\phi_0}|\theta-\theta_c|\right). \tag{2}$$

The singular behavior $\delta\rho_a^{(\rm s)} \sim |\delta\theta|$ in eq. (2) implies that the resistivity displays a sharp notch when θ is close to θ_c as observed. Let us consider the curve of R_{xx} (or ρ_a) *vs.* θ (fig. 4). As $\boldsymbol{H}$ is rotated in the plane b^*c^* normal to $\boldsymbol{a}$, R_{xx} displays a series of sharp notches [1]. At $\theta_c \simeq 4^\circ$, n_B vanishes in the ac plane. The restoration of long-range phase correlation in ac leads to a large rise in conductance observed as the steep decrease in R_{xx} in both figs. 2 and 4. As $\boldsymbol{H}$ deviates from θ_c, $\rho_c^{(\rm s)}$ increases steeply with $n_B \sim H|\delta\theta|$. When n_B gets so large that phase coherence in the ac plane is reduced to very short length scales, R_{xx} reverts to the dome-shaped background ($|\delta\theta| > 15^\circ$) (fig. 4). Similarly, the weak notch at the magic angle $\theta_{L1} \simeq 32^\circ$ occurs when $\boldsymbol{H}||(\boldsymbol{c}+\boldsymbol{b})$. The conductance increase is relatively modest because of the weak Josephson coupling in the plane $a(c+b)$. Finally, when $\boldsymbol{H}||\boldsymbol{b}$ (at θ_b), long-range phase coherence is restored in the strongly coupled plane ab, resulting in a deep notch in R_{xx}. (The notch at θ_{L1} is slightly weaker than that at $\theta_{-L1} \simeq -20^\circ$. The slight asymmetry reflects the slight bond-length difference ($|\boldsymbol{c}+\boldsymbol{b}| > |\boldsymbol{c}-\boldsymbol{b}|$) which implies a larger t along $\boldsymbol{c}-\boldsymbol{b}$.)

Implicit in our model is the surprising ability of the magnetic field to destroy phase coherence in the planes to which it is normal while enhancing conductivity in the planes to which it is parallel. It is natural that the vortices penetrating perpendicular planes destroy superconductivity. It is also natural that a field applied between two highly conducting/superconducting planes tends to decouple them by free flowing Josephson vortices as in the cuprate superconductors. However, in the present scenario, it is the *least* conducting planes which remain internally coherent and they remain decoupled from each other even though the interplane bandwidth (along $\boldsymbol{b}$) is more than an order of magnitude larger than the intraplane bandwidth (along $\boldsymbol{c}$). From the usual behavior of anisotropic superconductors, this magic-angle behavior seems rather counter-intuitive, although not precluded in principle.

A physical picture of superconductivity in this material is that it results from interactions within the chains, in which the p-wave pairing susceptibility is enhanced by the same spin fluctuations which cause a Mott insulating SDW at lower pressures. However, because of Coulomb blockade and localization effects, a strictly 1D chain is not superconducting as $T \to 0$. Hence conductivity must arise from interchain coupling. In weak fields, we have 3D superconductivity, but when interplane coupling is suppressed by $\boldsymbol{H}||\boldsymbol{b}$ or $\boldsymbol{c}$, the 2D planes

become resistive (they lie above their KT transition). The phase stiffness in the direction $\boldsymbol{b}$ is proportional to t_b^2/t_a and hence also small. Thus, the magic angles are, in a sense, where restoration of interchain coupling allows the current to bypass obstructions along the chains. In principle, this mechanism is similar to that proposed in Strong *et al.* [7].

In summary, we have shown that the angular Nernst signal in the "metallic" phase of $(TMTSF)_2PF_6$ is well accounted for in a model in which the Cooper pairing amplitude $|\hat{\psi}|$ remains finite, but superfluidity is absent because of dominant phase fluctuations produced by mobile vortices. When $\boldsymbol{H}$ tilts away from a principal plane direction, the sharp increase in 2D vortex density leads to a notch in the resistance as well as an angular Nernst signal of the observed magnitude.

* * *

We acknowledge discussions with Y. Wang and I. J. Lee. This research is supported by the US National Science Foundation (MRSEC Grant DMR 0213706) and DMR-0243001.

REFERENCES

[1] Kang W., Hannahs S. T. and Chaikin P. M., *Phys. Rev. Lett.*, **69** (1992) 2827; **70** (1993) 3091.
[2] For a review, see Chaikin P. M., *More is Different*, edited by Ong N. P. and Bhatt R. N. (Princeton University Press, Princeton) 2001, p. 151.
[3] Danner G. M. and Chaikin P. M., *Phys. Rev. Lett.*, **75** (1995) 4690.
[4] Chashechkina E. I. and Chaikin P. M., *Phys. Rev. Lett.*, **80** (1998) 2181.
[5] Lebed A. G., *JETP Lett.*, **43** (1986) 174; Lebed A. G. and Bak P., *Phys. Rev. Lett.*, **62** (1989) 1315.
[6] Osada T. *et al.*, *Phys. Rev. B*, **46** (1992) 1812; Yakovenko V. M., *Phys. Rev. Lett.*, **68** (1992) 3607; Chaikin P. M., *Phys. Rev. Lett.*, **69** (1992) 2831; Lebed A. G., *J. Phys. I*, **6** (1996) 1819.
[7] Strong S. P. *et al.*, *Phys. Rev. Lett.*, **73** (1994) 1007; Clarke D. G. *et al.*, *Science*, **279** (1998) 2071.
[8] Wu W., Lee I. J. and Chaikin P. M., *Phys. Rev. Lett.*, **91** (2003) 056601.
[9] For a review, see Kim Y. B. and Stephens M. J., in *Superconductivity*, Vol. **II**, edited by Parks R. D. (Dekker, New York) 1969.
[10] Wang Yayu *et al.*, *Phys. Rev. B*, **64** (2001) 224519.
[11] Emery V. J. and Kivelson S. A., *Nature*, **374** (1995) 434.
[12] Xu Z. A., Ong N. P., Wang Y., Kageshita T. and Uchida S., *Nature*, **406** (2000) 486.
[13] Wang Yayu *et al.*, *Phys. Rev. Lett.*, **88** (2002) 257003.
[14] Wang Yayu *et al.*, *Science*, **299** (2003) 86.
[15] Capan C. *et al.*, *Phys. Rev. Lett.*, **88** (2002) 056601.
[16] Ong N. P., Wang Yayu, Ono S., Ando Yoichi and Uchida S., cond/mat-0312213 (2003).
[17] Halperin B. I. and Nelson David R., *J. Low Temp. Phys.*, **36** (1979) 599.